Available online at www.sciencedirect.com
SCIENCE DIRECT®
Sensors and Actuators B 102 (2004) 59–66
SENSORS AND ACTUATORS B CHEMICAL
www.elsevier.com/locate/snb

Design and operation of a microfluidic sorter for *Drosophila* embryos

C.C. Chen [a,*], S. Zappe [a], O. Sahin [a], X.J. Zhang [a], M. Fish [b], M. Scott [b], O. Solgaard [a]

[a] *Department of Electrical Engineering, Stanford University, Stanford, CA 94305, USA*
[b] *Department of Developmental Biology, Stanford University, Stanford, CA 94305, USA*

Received 1 July 2003; received in revised form 1 July 2003; accepted 7 October 2003

Available online 21 January 2004

Abstract

We present measurements and simulation of fluid flow and sphere motion in a pressure-driven microfluidic sorter designed for *Drosophila* embryos. We simulate the flow fields for different channel layouts and study the effect of control pressure, chamber length and entrance length on switching time to find geometries and conditions for optimized embryo movement. We validate the sorter design with fluid experiments in devices fabricated from silicon and Pyrex wafers. The experimental and simulated results are compared both qualitatively and quantitatively by examining the concentration distribution of fluids. This type of microfluidic sorter is promising for micromanipulation of a variety of biological cells, and provides automated operations for higher throughput and accuracy.

Keywords: Microfluidic; Micromanipulation; Sorter; Switching time

1. Introduction

Microfluidic devices fabricated by microelectromechanical systems (MEMS) technology are becoming prevalent in biological and medical applications. An important application is sorting of cells and embryos in devices that combine fluidics, mechanics, optics and electronics to identify, manipulate, and sort large numbers of individual cells or embryos [1]. Several research groups have reported microfluidic cell sorters using electrophoresis, electro-osmosis and pressure to manipulate cells and reagents [2–4]. Computer-aided design tools can facilitate and accelerate microsystem implementation, but the ability of computational fluid dynamics to simulate the flow of cellular particles (cells, embryos, bacteria, viruses) is underdeveloped [5]. In this paper, we describe the design, simulation, fabrication and experimental verification of an off-chip-controlled microfluidic switch for cell and embryo sorting.

2. Microfluidic switch design

The structure of the embryo sorter is shown schematically in Fig. 1. We change the pressure of the two control inlets to direct the main flow and cells to outlet$_1$ or outlet$_2$. Our method of manipulating cells is based on the ability of the cells to follow the flow due to drag forces. The flow is usually laminar in microchannels, so unwanted turbulence does not impede our ability to control the fluid flow. Whether the flow is laminar or turbulent can be determined by the Reynolds number ($Re = UD/\nu$, where U is the velocity of the fluid, D is the dimension of the channel, and ν is the kinematic viscosity). In our study, Re numbers range from 1 to 500 with different volumetric flow rates. The experimental data of Wu and Little on glass and silicon microchannels indicate that for $Re < 1000$ the flow is laminar, for $1000 < Re < 3000$ the flow is in the transition region, and for $Re > 3000$ the flow is fully turbulent [6].

3. Microfluidic simulation

The flow dynamics of our microfluidic cell switch is analyzed with the CFD-ACE+ software [7]. The present study employed transient incompressible fluid flow and the volume-of-fluid (VOF) method for free-surface flows with surface tension. The fluid-flow model solves the time dependent continuity equation, the pressure-based Navier–Stokes equations, and the energy balance equation. Grid independence tests were performed for the 3D grid system used in the simulation and the final grid cell node number was 36,448.

Fig. 2(a) shows the steady-state pressure and velocity distributions with the pressure of the control$_1$ (P_1) and cell (P_C)

* Corresponding author. Tel.: +1-650-724-4654; fax: +1-650-725-2533.
E-mail address: chungchu@stanford.edu (C.C. Chen).

0925-4005/$ – see front matter © 2003 Elsevier B.V. All rights reserved.
doi:10.1016/j.snb.2003.10.015

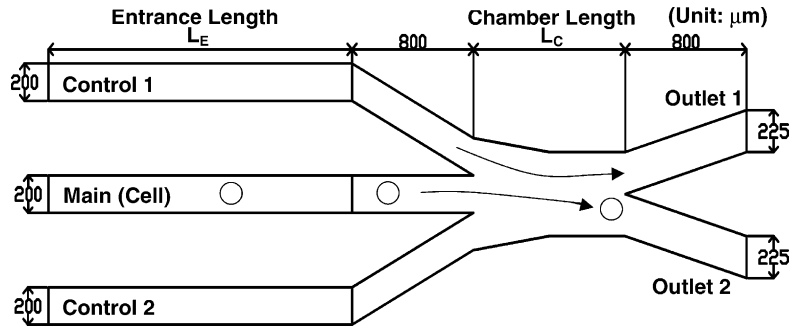

Fig. 1. Geometry and dimensions of the simulated fluidic cell switch.

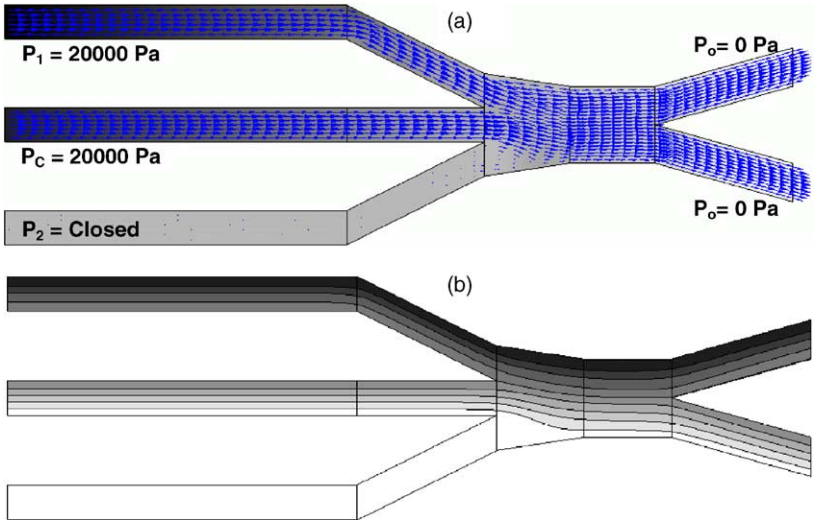

Fig. 2. Steady-state simulations of (a) pressure and velocity distribution, and (b) stream function.

inlets maintained at 20,000 Pa, and control$_2$ (P_2) closed. This condition directs all the fluid from the cell inlet to outlet$_2$, as shown in the stream function map of Fig. 2(b).

Fig. 3 shows results of 3D computations of the operation of the microfluidic sorter with floating embryos. The simulated embryo consists of fluid with higher surface tension that tends to minimize surface area. Thus a spherical shape is maintained. As predicted, spheres of a size comparable to the channels followed the fluid flow fairly well. However, the cells have an obstructive effect on the flow. As shown in the color map of the pressure distribution in Fig. 3, the volume behind the embryos exhibits a higher pressure than the surroundings.

4. Switch dynamics

Fig. 4 shows three instances of transient results of the fluid switching from outlet$_2$ to outlet$_1$ for the microfluidic switch with dimensions shown in Fig. 1 and a control pressure of 40,000 Pa. The switching time is 360 μs and is measured from the instant that the pressure changes in control inlets to the instant that the main flow switches totally from one outlet to the other. A switching length of 540 μm is found by multiplying the switching time and the flow velocity (1.5 m/s on average) in the central channel. Cell detection and decision must, therefore, be made at least 540 μm upstream of the switch fork point shown in Fig. 4.

The switching time of the microfluidic switch is a function of geometry/dimension, control pressure, and the properties of the working fluids. Acceptable working fluids are determined by the cells to be sorted, according to toxicity, compatibility and density [8]. The fluid should not interfere with cell identification and should be easy to separate from the cells. The viscosity of the fluid is essential to the flow inside the micro channels, but in this paper only aqueous solutions will be considered. The control pressure and switching chamber length were varied in our simulation to investigate their effects on the switching time. We also simulated different entrance length to check the delay of the switching caused by additional channel length. The parameters used in the study of switching time are listed in Table 1.

Fig. 5 shows the switching time, T_{SW}, with four different control pressures. The switching time drops from 796 to 360 μs nonlinearly with increasing pressure from 9000 to 40,000 Pa. The functional relation between T_{SW} and P can be

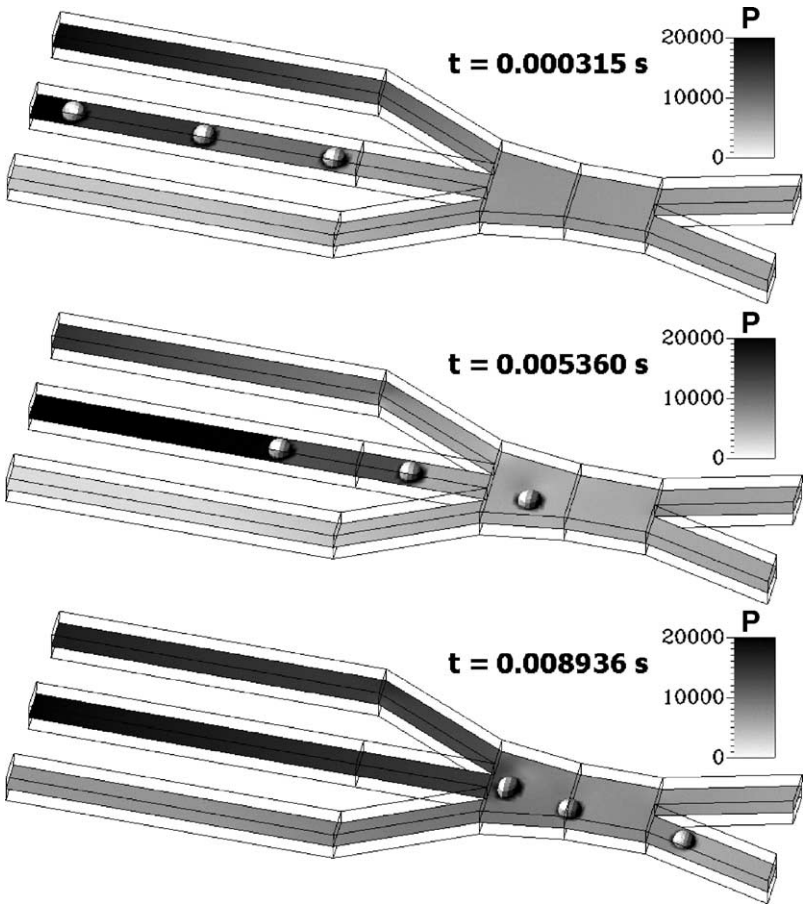

Fig. 3. Three-dimensional simulation of cell movement in the cell switch.

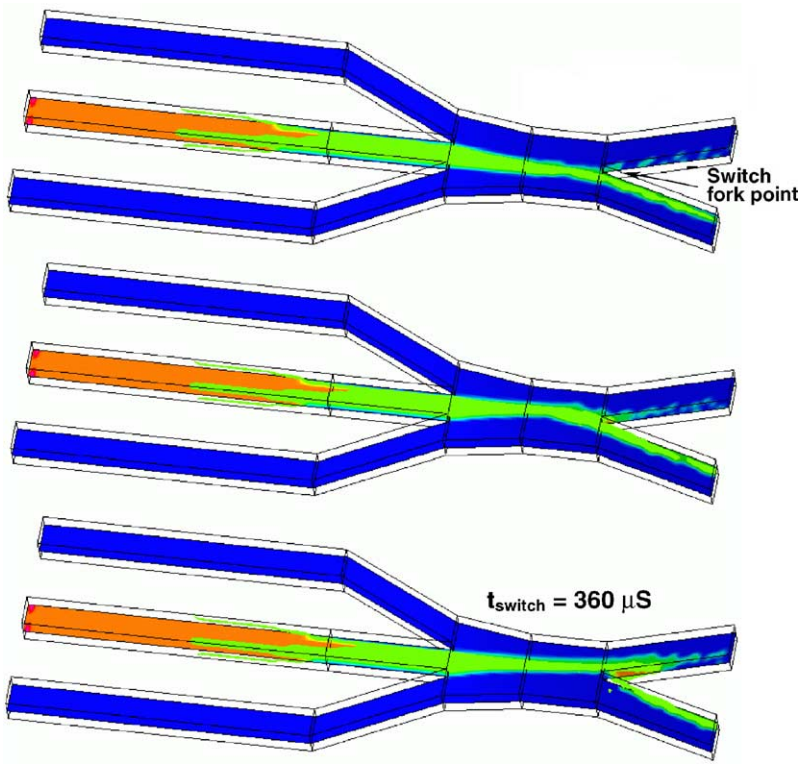

Fig. 4. Simulated fluid switching (from $outlet_2$ to $outlet_1$) for control pressure of 40,000 Pa.

Table 1
Parameters used in the switching time study

Case	P (Pa)	L_C (μm)	L_E (μm)
Control pressure	9000	1000	1500
	10000		
	20000		
	40000		
Chamber length	20000	250	1500
		500	
		1000	
		1500	
Entrance length	20000	1000	1500
			2000
			3000
			4500

expressed as $T_{SW} = 98381P^{-0.5307}$. Increasing the control pressure over 40,000 Pa will reduce switching time, but will also results in higher velocity and eventually turbulent flow. Our simulations show that the Reynolds number reaches the onset value for turbulence at 160,000 Pa control pressure. Beyond this pressure, the switch will not function properly because it relies on switching of laminar flows.

Fig. 6 shows the relationship between the chamber length, L_C, and the switching time, T_{SW}, with the control pressure maintained at 20,000 Pa and the entrance length at 1500 μm. The switching time increases linearly from 360 to 650 μs when the chamber length is increased from 500 to 1500 μm. However, the switching time increases slightly when L_C is reduced to 250 μm. This is because the switch fork is too close to the convergence area of the three inlets, as shown in Fig. 7(a). This has a detrimental effect on the flow through the switch. The 500 μm chamber is long enough for the switching flow to develop, and provides the optimized switching time of 357 μs, as shown in Fig. 7(b).

Fig. 8 shows the time delay, ΔT, contributed by the additional entrance length, ΔL_E. The parameters ΔL_E and ΔT are calculated from the values of L_E and T_{SW} with the baseline values (1500 μm and 506 μs, respectively) subtracted. The relationship between ΔL_E and ΔT is quite linear and can be represented by $\Delta T = 0.1114\ \Delta L_E$ for entrance lengths from 1500 to 4500 μm.

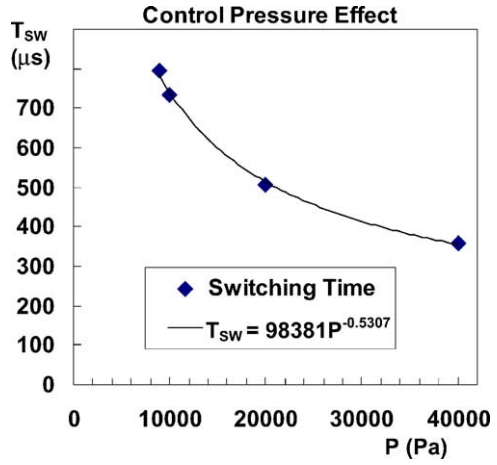

Fig. 5. Effect of control pressure on the switching time, T_{SW}.

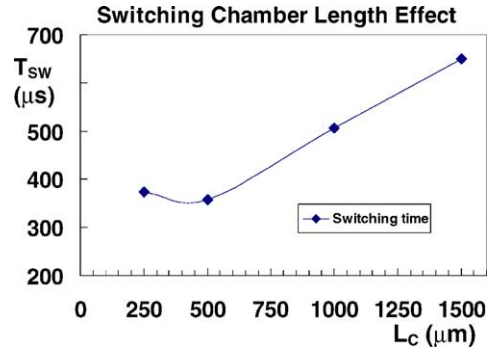

Fig. 6. Effect of chamber length on the switching time, T_{SW}.

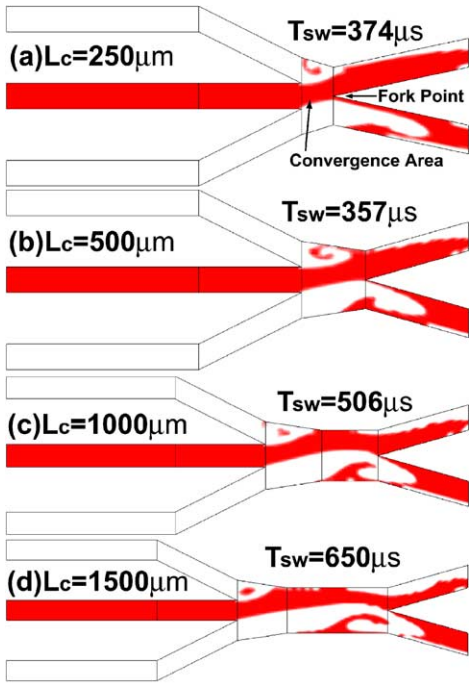

Fig. 7. Simulated fluidic switching with varying chamber length.

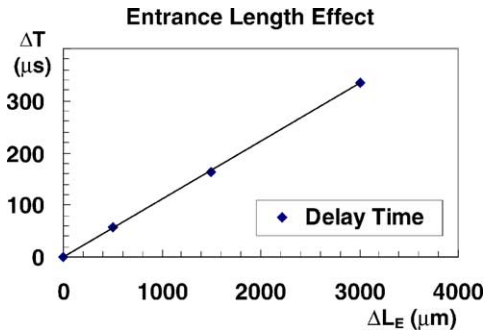

Fig. 8. Effect of entrance length on switching delay (ΔT).

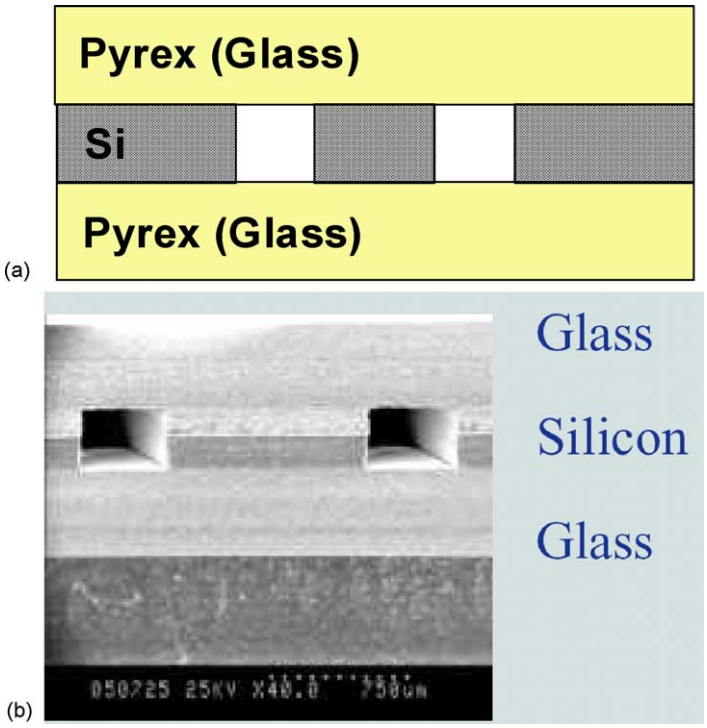

Fig. 9. Schematic drawing and SEM of the fabricated microfluidic switch.

5. Device fabrication

Pyrex (glass) wafers were used as top and bottom covers of the microfluidic switch to provide optical access of the laser light source and the photo detector. Amorphous silicon (a-Si) layers are deposited on both sides of the Pyrex wafer to form protective layers against hydrofluoric acid (HF). The a-Si layers were patterned in a dry etch, and HF was used to etch through the Pyrex wafers. The etched holes provide connections to the microfluidic channels. The a-Si layers were then removed in potassium hydroxide (KOH) before cleaning the Pyrex in hydrogen chloride (HCL), hydrogen peroxide (H_2O_2), and sulfuric acid (H_2SO_4)/H_2O_2. The silicon wafer was patterned using standard photolithography and was dry-etched by deep reactive ion etching to form the microfluidic channels. After patterning, the silicon wafer was thinned to 360 μm, and the Pyrex wafers were anodically bonded to its top and bottom, as illustrated in Fig. 9(a), to complete the microfluidic channels and provide optical access and fluid connections. A scanning electronic microscope image of the fabricated micro channels is shown in Fig. 9(b).

6. Experimental verification

The optical measurement set-up depicted in Fig. 10 was used to characterize and verify the function of the microfluidic sorter. A control fluid with red (dark) dye was used both for flow visualization, and as a laser light block so the flow could be recorded on the photo detector.

Fig. 11 shows good consistency in the qualitative comparison between the simulated (a) and video-captured (b) flow patterns, except within a recirculation zone where some low-speed dark fluid is surrounded by transparent fluid, as shown by the upper right inset in Fig. 11(a). In the experiment, the transparent fluid tends to push the dark fluid back toward the inlet of control$_2$, as shown in the inset of Fig. 11(b). We believe this phenomenon is due to the fluidic

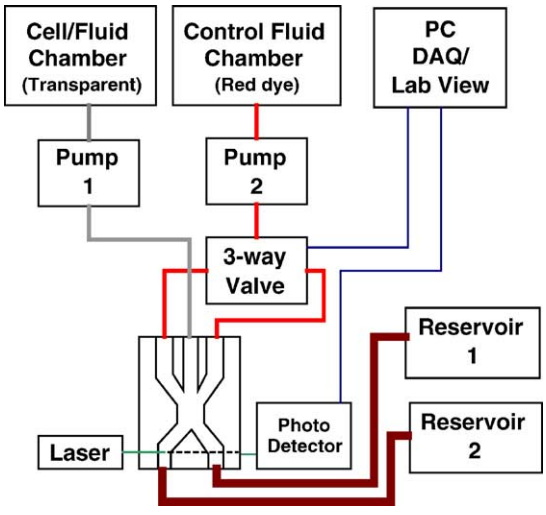

Fig. 10. Schematic setup of cell switch experiment.

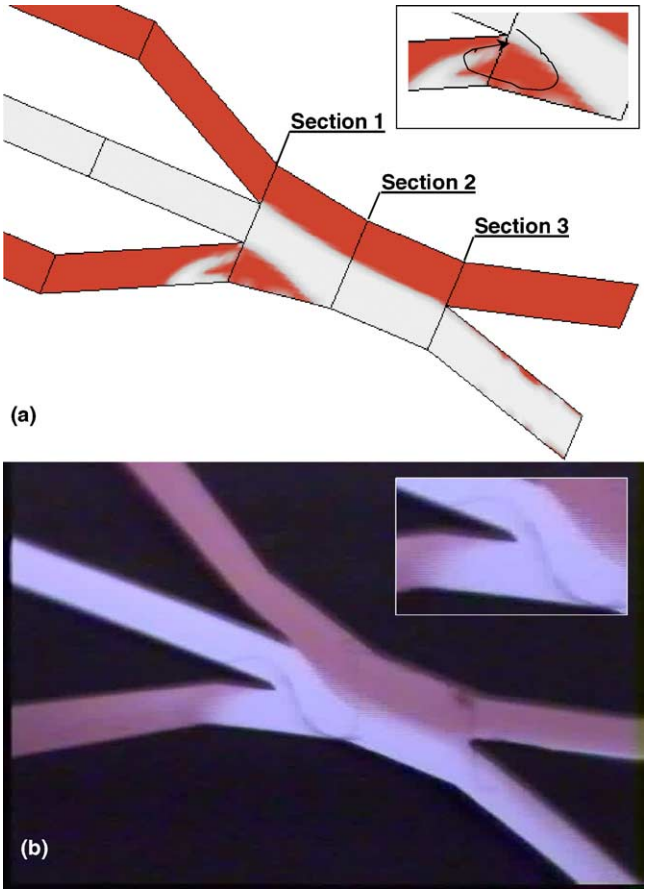

Fig. 11. Comparison of (a) simulated and (b) video-captured flow visualizations of the cell switch.

capacitance effect of the flexible tube connecting the microfluidic switch and the control valve. This effect needs further study before it can be taken into considerations in the simulations.

Quantitative comparisons between experimental and simulated results were made in three selected cross-sections shown in Fig. 11(a). The normalized light intensity, I^*, in video-captured image can be calculated by the formula:

$$I^* = \frac{I - I_{\min}}{I_{\max} - I_{\min}}$$

where $I_{\max}$ and $I_{\min}$ are the maximum and minimum value of light intensity transmitted through the flow channel. The normalized light intensity represents the concentration of the transparent fluid (main fluid) in the experiment. Fig. 12 shows the comparison of these values to the volume fraction, F, extracted from the simulation results. The parameter F specifies the fraction of the volume of each computational grid occupied by main fluid (transparent) while $1 - F$ represents values of the secondary fluid (dark). Fig. 12 depicts the F and I^* curves in the three selected cross-sections. As noted earlier, there is a prominent discrepancy between simulation and experiment at $Y = -120$ to 280 μm in Section 1. Outside this region, as evidenced in the cross-sectional curves

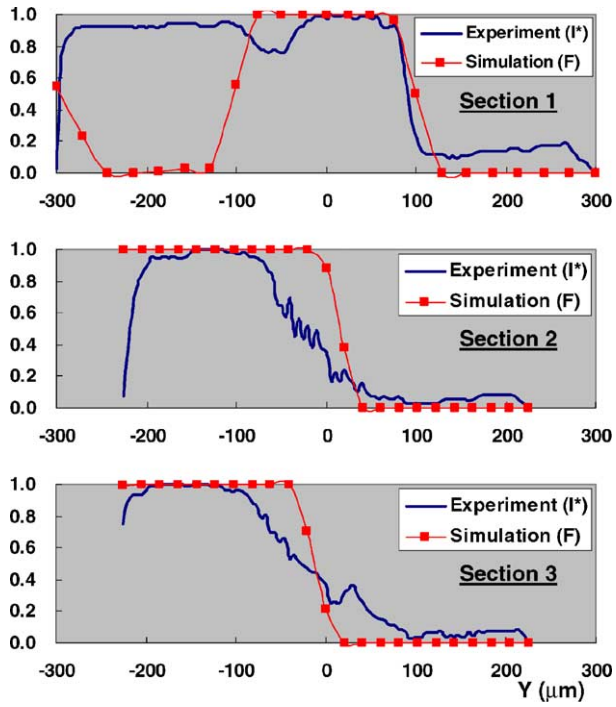

Fig. 12. Quantitative comparison of normalized light intensity I^* (experiment) and volume fraction F (simulation).

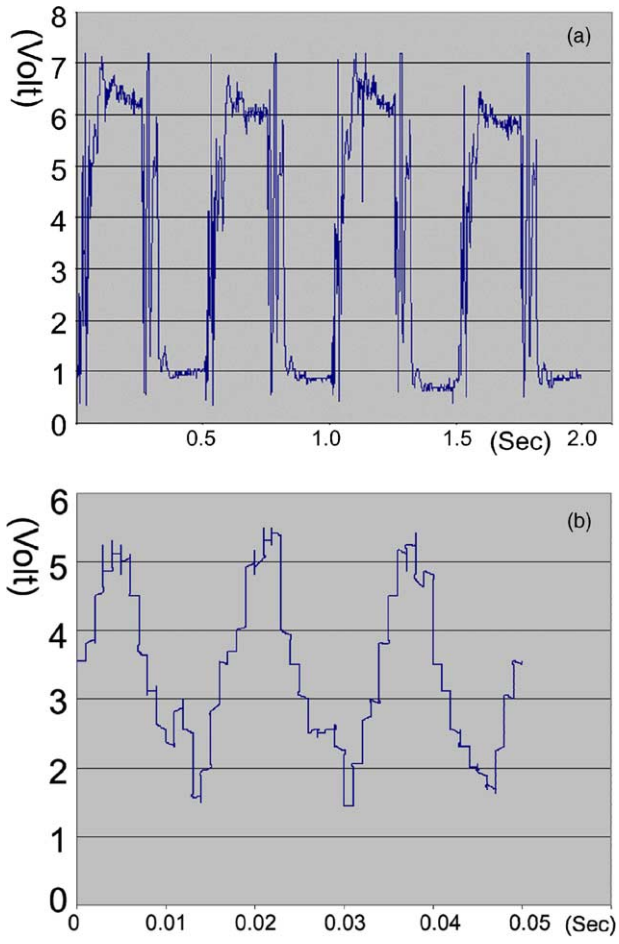

Fig. 13. Detector readout of the fluid switching at (a) 2 Hz and (b) 60 Hz.

in Fig. 12(b and c), the simulations and experiments are well matched except for the lower concentration gradients near the fluid interface caused by more mixing in the experiment.

The dynamics of the switching process was studied by changing the switching frequency. Fig. 13 shows representative detector voltage readouts for 2 Hz (a) and 60 Hz (b) periodic switching. The response at 60 Hz is in good agreement with the response time of 5 ms of the electromagnetic three-way valve used to control the pressure. This shows that the switch works well up to switching speeds of this magnitude. To verify the simulated switching times that ranges from 360 to 796 μs, a faster pressure valve is needed.

7. Conclusions

In this paper, we have demonstrated the design, simulation, fabrication and operation of a microfluidic switch for embryo and cell sorting. An off-chip pressure-driven control technique was used to hydrodynamically switch the fluid between different micro channels. Finite volume simulation software was used to verify the concept and to optimize the design. The effects of control pressure, chamber length and entrance length on the switching time were investigated. The switching time drops nonlinearly with increasing control pressure as $P^{-0.53}$. Simulations show that the pressure can be increased to 160,000 Pa before turbulence compromises the operation of the switch. The optimized chamber length is 500 μm and provides the shortest switching time of 357 μs with a control pressure of 20,000 Pa. The switching delay varied linearly with entrance length in the range of 1500–4500 μm.

To verify the simulations, a microfluidic switch was fabricated and optical measurements were taken and compared to the simulation results. The concentration distributions of fluids were extracted from experiment and simulation data. Good qualitative correspondence between experiments and simulations was found throughout the active volume of the fluidic switch, and good quantitative correspondence was found in three cross sections that were analyzed in detail. The switching time of the experimental system is limited by the response time of 5 ms of the electromagnetic three-way valve used to control the pressure.

Acknowledgements

Support for this research was provided by the Defense Advanced Research Projects Agency under contract MDA972-00-1-0032.

References

[1] E.E.M. Furlong, D. Profitt, M.P. Scott, Automated sorting of live transgenic embryos, Nat. Biotechnol. 19 (2001) 153.

[2] A.Y. Fu, C. Spence, A. Scherer, F.H. Arnold, S.R. Quake, A microfabricated fluorescence-activated cell sorter, Nat. Biotechnol. 17 (1999) 1109.

[3] S. Gaward, L. Schild, P. Renaud, Micromachined impedence spectroscopy flow cytometer for cell analysis and particle sizing, Lab. Chip 1 (2001) 76.

[4] K.D. Kramer, K.W. Oh, C.H. Ahn, J.J. Bo, K.R. Wehmeyer, An optical MEMS-based fluorescence detection scheme with applications to capillary electrophoresis, SPIE-Microfluidic Devices Syst. 3515 (1998) 76.

[5] A. Przekwas, Multiphysics, multiscale design tools for microfluidic biochips with electronic and optical readout, in: Symposium on Design Test Integration and Packaging of MEMS/MOEMS, Cannes, France, May 1–3, 2002.

[6] P. Wu, W.A. Little, Measurement of heat transfer characteristics of gas flow in fine channel heat exchangers used for microminiature refrigerators, Cryogenics 24 (8) (1984) 415–420.

[7] CFD-ACE+ Software Manuals, CFD Research Corp., USA, 2002.

[8] D. Patel, Separating Cells, BIOS Scientific Publishers Ltd., Oxfordshire, UK, 2001, pp. 49–68.

Biographies

Chung-Chu Chen received the B.Sc. degree in mechanical engineering from National Taiwan University, Taiwan, in 1994 and the Ph.D. degree in power mechanical engineering from National Tsing Hua University, Taiwan in 1999. He worked as an engineer with Microsystem Technology Division, Electronics Research and Service Organization (ERSO) of the Industrial Technology Research Institute (ITRI), Taiwan, between 2000 and 2002. He is currently a Postdoctoral Researcher in Stanford University and is conducting his research at E. L. Ginzton Labs. His current research focuses on microfluidic device design, simulation, fabrication and characterization for several applications including cell sorting, fluid dispensing, micro droplet injecting and device cooling and he holds three related patents.

Stefan Zappe received his Diploma degree in electrical engineering from the Berlin University of Technology, Germany, in 1996. From 1996 until 2001 he worked as a Ph.D. student at the Microsensor and Actuator Center at the Berlin University of Technology. In February 2001, he joined the Stanford Microphotonics Laboratory at Stanford University, CA, USA as a Postdoctoral Researcher. His research activities include microfluidic systems for cell- and embryo-handling, sorting and micro-injection; biology of fruit fly development; gene silencing by means of RNA interference (RNAi); micro-orifices for DNA shearing; microfluidic systems based re-usable arrays for DNA sequencing; integration of active and passive optical components into microsystems.

Ozgur Sahin received his B.Sc. degree in electrical engineering from Bilkent University, Ankara, Turkey in 2001 and M.Sc. degree from Stanford University, CA, USA, in electrical engineering in 2003. He is currently working towards his Ph.D. degree in electrical engineering at Stanford University, CA, USA. His research interests include sensors based on nanomechanics and nanooptics and manipulation of cells within microfluidic systems. He is a student member of IEEE.

Xiao Jing(John X.J.) Zhang received his B.Sc. degree in precision electronic instrumentation from Shanghai Jiao Tong University, China in 1995 and his M.Sc. degree in electrical engineering from University of Maine, Orono in 1998. His industrial experience includes working at Hewlett-Packard (later, Agilent Technologies) on the design of parallel optical interconnects and the evaluation of IEEE802.3ae optical transceivers for Cisco 10 Gb/s LAN-switching equipment. He is currently a Ph.D. candidate in electrical engineering at Stanford University. His dissertation research includes diffractive optical microelectromechanical

systems (MEMS) and Bio-MEMS design, fabrication and characterization, with focus on developing integrated microphotonic sensing platform for *in vivo* single cell and embryo manipulation, force microscopy and near-field imaging.

Matthew P. Fish received his B.Sc. degree in biology from San Jose State University, San Jose, CA, USA, in May 1991 and his M.Sc. degree in molecular biology from San Jose State University in May 1999. He is currently employed by the Howard Hughes Medical Institute, working at Stanford University, Stanford, CA, USA, in the department of developmental biology. His research work focuses on the function of a novel, developmentally regulated gene in *Drosophila melanogaster*.

Matthew P. Scott received his B.S. and Ph.D. degrees in biology from M.I.T. He did postdoctoral research at Indiana University and then joined the faculty at the University of Colorado at Boulder. In 1983, he moved to Stanford University School of Medicine where he is now Professor of Developmental Biology and of Genetics. He has published more than 130 papers and three patents. His research areas are developmental genetics and cancer research, particularly the roles of signaling systems and transcriptional regulation in embryonic development. His research employs genetics, genomics, cell biology, and molecular biology in exploring how cells acquire their fates and are patterned. He is an editor of *Current Opinion in Genetics and Development* and of the *Proceedings of the National Academy of Sciences*. He is a past president of the Society for Developmental Biology, a member of the American Academy of Arts and Sciences, and a member of the National Academy of Sciences. He is presently chairing Stanford's Bio-X program, which is designed to accelerate the coming together of engineering, physics, and chemistry with biology and medicine.

Olav Solgaard received his B.S. degree in electrical engineering from the Norwegian Institute of Technology and his M.S. and Ph.D. degrees in electrical engineering from Stanford University, California. He held a postdoctoral position at the University of California at Berkeley, and an assistant professorship at the University of California at Davis, before joining the faculty of the Department of Electrical Engineering at Stanford University in 1999. His research interests are optical communication and measurements with an emphasis on semiconductor fabrication and MEMS technology applied to optical devices and systems. He has authored more than 100 technical publications, and holds 13 patents. He is a co-founder of Silicon Light Machines, Sunnyvale, CA, USA, and an active consultant in the MEMS industry.